Pergamon

PII: S0043-1354(96)00141-8

Wat. Res. Vol. 30, No. 11, pp. 2761–2765, 1996

0043-1354/96 $15.00 + 0.00

LIQUID FLOW AND MASS TRANSPORT IN HETEROGENEOUS BIOFILMS

DIRK DE BEER, PAUL STOODLEY and ZBIGNIEW LEWANDOWSKI*

Center for Biofilm Engineering, 409 Cobleigh Hall, Montana State University, Bozeman, MT 59717, U.S.A.

(First received May 1995; accepted in revised form April 1996)

Abstract—Convective mass transport in heterogeneous biofilms, consisting of cell clusters and voids, was investigated using oxygen microelectrodes. Oxygen concentration profiles were measured and contour plots constructed at different (average) flow velocities (U_{avg}). The profiles were used to determine the thickness of the mass transfer boundary layer (δ_h) above the voids and the cell clusters. The δ_h above the biofilm was inversely related to flow, as expected, and decreased exponentially with increasing flow velocity. However, the δ_h above the voids decreased more rapidly than the δ_h above the cell clusters resulting in two distinct situations; at low flow velocities the oxygen contours were parallel to the substratum but at high velocities were parallel to the irregular biofilm surface. It was concluded that at low flow velocities the biofilm could be modeled one-dimensionally, with fluxes perpendicular to the substratum and the exchange area being equal to the substratum area, but at higher velocities biofilm voids facilitate mass transport and a more complex, three-dimensional model would be more appropriate. In this latter case fluxes are multidirectional, and the exchange area is equal to that of the convoluted biofilm surface. Copyright © 1996 Elsevier Science Ltd

Key words—biofilm structure, mass transfer boundary layer, convection, mass transport

INTRODUCTION

Mass transport can have a significant influence on the rate of various biotransformation reactions occurring in biofilm systems since it is often the rate limiting process (Characklis *et al.*, 1990a). Therefore, to fully understand and optimize processes occurring in natural and industrial biofilms it is necessary to determine the rates of both diffusive and convective mass transport. Although it has been recognized that biofilms are structurally heterogenous the description of mass transport is generally based on a planar biofilm model in which transport processes are divided into two regions: a) the bulk liquid in which convection is considered the significant mass transfer process, and b) the base biofilm compartment in which only molecular diffusion occurs (Lewandowski *et al.*, 1991; Rittman and Manem, 1992; Siegrist and Gujer, 1985). Recent application of confocal scanning laser microscopy (CSLM) to biofilm research has shown that biofilms can have a complex structure consisting of cell clusters, discrete aggregates of microbial cells in an EPS matrix, and interstitial voids, open channels connected to the bulk liquid (De Beer *et al.*, 1994a; Lawrence *et al.*, 1991; Massol-Deya *et al.*, 1995). Additionally, the combination of CSLM with microelectrode measurements has allowed the effect of structural heterogeneity on hydrodynamics and mass transport to be more carefully studied. Microelectrode measurements showed that oxygen concentrations in the voids were significantly higher than in the adjacent cell clusters, demonstrating that voids can act as transport channels (De Beer *et al.*, 1994a). Liquid flow through the voids was directly demonstrated and quantified by dye and particle tracer studies (De Beer *et al.*, 1994b; Stoodley *et al.*, 1994). The intra-film velocity was directly related to the average velocity of the bulk liquid (U_{avg}), however, the liquid in the cell clusters appeared stagnant. Consequently, it was concluded that in cell clusters molecular diffusion is the predominant transport mechanism while in voids both diffusion and convection are possible. Since the intra-biofilm liquid flow depended on U_{avg}, convection is expected to be increasingly important as the flow velocity increases.

The influence of the bulk liquid flow velocity on convection in the voids can be interpreted from interfacial transport phenomena. In a biofilm system substrate transport involves convection from the bulk liquid to the near vicinity of the cell clusters, diffusion through the mass transfer boundary layer, and diffusion through the cell clusters to the cells. The thickness of the mass transfer boundary layer δ_h can be estimated graphically by linearly extrapolating the maximal substrate gradient (in a planar biofilm at the biofilm surface) to the bulk liquid concentration, δ_h being the distance between the intercept and the biofilm surface (Kashe and Kuhlman, 1980). The

*Author to whom all correspondence should be addressed [Tel.: 406-994-4770; Fax: 406-994-6098].

concentration difference between the bulk liquid and the biofilm surface, the diffusion coefficient of the solute (D_s), and δ_h determine the diffusive solute flux to the biofilm. It is well known that the thickness of the mass transfer boundary layer is influenced by U_{avg}, δ_h becoming smaller at higher U_{avg}. However, the effects of an accumulated heterogenous biofilm on the profile shape of the mass transfer boundary layer has never been directly demonstrated. Since liquid does not flow through the cell clusters, biofilms may increase the roughness of a surface and, by changing the hydraulic regime, may reduce the δ_h (Characklis, 1973). Although biofilm roughness has been recognized in a number of studies on bioreactors, its influence on mass transfer has not been incorporated in mathematical models (Bryers, 1987; Diks and Ottengraf, 1991a, b; Howell and Atkinson, 1976). Agreement between models and experimental data can be achieved by manipulating the intrinsic kinetic parameters, by adapting the area of active biofilm or by neglecting the external and/or internal mass transfer resistance (Diks and Ottengraf, 1991a, b; Skowland and Kirmse, 1989). Such approaches have obvious limitations. Additionally, an irregular biofilm surface may cause local variations in the thickness of the mass transfer boundary layer, δ_h being larger in the voids between the cell clusters than above them. Jorgensen *et al.* (1990) found in sediments that the mass transfer boundary layer (for that study defined as the point of 90% air saturation) followed the surface elements only if the thickness of the roughness elements were greater than 50% of the thickness of the mass transfer boundary layer. The surface area for substrate and product exchange between the biofilm and the bulk liquid is determined by the profile of the mass transfer boundary layer. If the mass transfer boundary layer is parallel to the substratum, the exchange area is equal to that of the substratum surface area. However, if the mass transfer boundary layer is convoluted (follows the irregular biofilm surface) the exchange area can be greatly increased and, as a result, the mass transport rate between the bulk fluid and the biofilm may also be increased.

In this study the significance of convective mass transport within biofilms was assessed. If convection in voids occurs, the substrate concentration difference between voids and cell clusters is expected to increase with increasing U_{avg}. To evaluate the role of convection, oxygen microprofiles in voids and cell clusters were measured at various flow velocities with oxygen microelectrodes in a biofilm grown with oxygen as the limiting substrate.

MATERIALS AND METHODS

Biofilm reactor

The reactor system, consisted of a polycarbonate closed channel (0.5 cm wide, 1.0 cm deep) flow cell in a recycle loop which also included an aeration/mixing chamber and recirculation pumps. The flow cell had a rectangular glass coverslip viewing port (60 × 24 mm) 15 cm from the inlet. Biofilm growing on the coverslip could be microscopically examined *in situ* and was accessible for specially designed "J" shaped oxygen microelectrodes (De Beer *et al.*, 1994a). The reactor was initially filled with a minimal salts medium (2.2 mM KH_2PO_4, 4 mM K_2PO_4, 0.76 mM $(NH_4)_2SO_4$, 4.1×10^{-2} mM $MgSO_4$, and 2.2 mM glucose) and inoculated with frozen stock cultures of *Klebsiella pneumonia*, *Pseudomonas fluorescens* and *Pseudomonas aeruginosa*. The reactor was run in batch mode for 6 h to allow colonization of the coverslip and subsequently was switched to continuous culture with a liquid residence time of 26 min and recycle flow rate of 4.5 ml/s (U_{avg} = 9.5 cm/s). The biofilm was allowed to grow until it was around 175 μm thick (4–5 days) and all of the experiments were performed at 20 + 1°C. The reactor system is described in more detail in previous publications (De Beer *et al.*, 1994a, b).

Microelectrode measurements

Oxygen profiles were measured at various flow velocities using "J" shaped microelectrodes, with 5–10 μm tips, prepared as described previously (De Beer *et al.*, 1994a). Oxygen profiles were measured at 50 μm intervals along transects, ranging from 500 to 1000 μm in length, traversing both voids and cell clusters. A regular matrix of data points was constructed from the profiles by linear interpolation. Subsequently, contour plots were made showing lines of equal oxygen concentration. Oxygen concentration in the flow cell was influenced by the flow rate (under constant aeration rate) because of the development of axial oxygen concentration gradients due to oxygen consumption by biofilm in the flow cell and recycle tubing. The oxygen concentration in the flow cell ranged from 0 mol/m^3 at flow rates below 0.01 m/s to 0.18 mol/m^3 at a flow rate of 0.12 m/s. To overcome this effect the system was purged with pure oxygen to maintain a concentration in the flow cell of 0.08(+0.006) mol O_2/m^3 during microelectrode measurements. At the highest flow velocity (0.115 m/s) the oxygen concentration could not be regulated well and increased to 0.18 mol/m^3.

Confocal microscopy

The structure of the biofilm was visualized by scanning laser confocal microscopy (Bio-Rad MRC600 attached to an Olympus BH2 microscope) using various microscopic techniques (De Beer *et al.*, 1994a): 1) fluorescence exclusion with fluorescein (0.1 mM) using an excitation wavelength (Ex) of 488 nm (Caldwell *et al.*, 1992); 2) reflected laser imaging (Ex = 488, 568, and 647 nm); and 3) biofilm autofluorescence (Ex = 568 nm).

RESULTS

After 4–5 days the biofilm consisted of cell clusters of 150–200 μm thickness separated by interstitial voids, the void fraction (of the substratum area) was approximately 50%. The substratum in between the cell clusters was covered with a 10–20 μm thick base film.

Oxygen concentration profiles were measured at various bulk liquid flow rates. When the flow velocity was low (0.0078 m/s) the oxygen profiles above the void and cell cluster areas were the same (Fig. 1A and B). The strongest gradients occurred between the depths of 120 and 230 μm. The vertical position of the mass transfer boundary layer (determined graphically, see Fig. 1A and B) was 240 μm from the substratum. The thickness of the mass transfer boundary layer (δ_h) was approximately 220 μm in the voids and 70 μm above the cell clusters. As the bulk

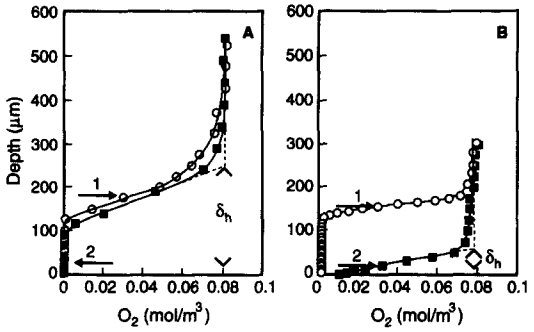

Fig. 1. Oxygen profiles at U_{avg} of 0.0078 m/s (A) and 0.064 m/s (B), over cell clusters (○) and void (■) areas. The dotted lines indicate extrapolations from the largest gradient and the bulk concentration. The arrows indicate the position of the upper surface of the cell clusters (1) and the base film (2).

velocity was increased the δ_h decreased both above voids and cell clusters (Fig. 2). However, the δ_h above the voids decreased more rapidly than the δ_h above the cell clusters and they were both approximately 50 μm at a bulk velocity of 0.04 m/s. Increasing the bulk velocity further caused the δ_h above voids and cell clusters to become asymptotic to the x-axis as δ_h approached zero.

The effects of velocity on the shape of the mass transfer boundary layer were clearly seen when contours of equal oxygen concentration were constructed from measurements made in a matrix over a X–Z plane (Fig. 3). At an U_{avg} of 0.0078 m/s the contours were parallel with the substratum, but at 0.115 m/s they closely followed the irregular biofilm surface. The strongest gradients were perpendicular to the substratum at the low velocities but were perpendicular to the irregular biofilm surface at the higher velocities.

DISCUSSION

The oxygen profiles and contour plots showed that the oxygen distribution depended on the velocity of the bulk liquid. At low U_{avg} (< 0.04 m/s; Fig. 3A) the oxygen contours were approximately parallel with the substratum surface, while at high U_{avg} (> 0.04 m/s; Fig. 3B) they followed the biofilm surface. The thickness of the mass transfer boundary layer above the void areas and cell clusters decreased exponentially with increasing velocity, becoming asymptotic with the x-axis as δ_h approached zero. The δ_h decreased more rapidly above the void areas than the cell clusters so that δ_h closely followed the irregular biofilm surface at the higher velocities. In the void areas oxygen depletion occurred away from the base film, close to the level of the top of the cell clusters (170μm depth) and was probably caused by lateral oxygen transport to the cell clusters, taking place within the boundary layer above the biofilm. It was concluded that under such conditions heterogeneous biofilms behave as though they were planar homogeneous structures and molecular diffusion the principal internal mass transport mechanism. In this case the dominant substrate fluxes are perpendicular to the substratum and the biofilm can be modeled using the conventional one-dimensional models.

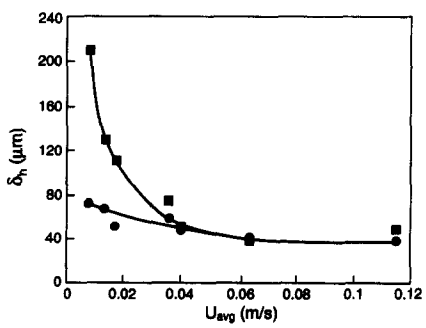

Fig. 2. Empirical relationship between the thickness of the mass transfer boundary layer, δ_h, and the average flow velocity, U_{avg}, above clusters (●) and voids (■).

However, as U_{avg} is increased and the mass transfer boundary layer becomes convoluted and parallel to the irregular biofilm surface, horizontal (parallel with the substratum) fluxes become an increasingly significant component of the total substrate flux into the biofilm. Also, since the mass transfer boundary layer approximates the effective exchange area, substrate transport is increased at higher U_{avg} because δ_h is decreasing and the effective exchange area is enlarged. In this case three-dimensional models could more accurately describe mass transport processes. The contribution of biofilm voids to the total mass transport was evaluated by comparing oxygen transport rates (1) from the bulk liquid into the cell clusters, (2) from the voids into the cell clusters, and (3) from the voids into the base film. Diffusive fluxes across each of the three interfaces were calculated from the horizontal and vertical concentration gradients at the relevant interface using Fick's first law, assuming D_s for oxygen of 2.27×10^{-9} m^2/s (De Beer *et al.*, 1994a). The oxygen fluxes from the voids to the cell clusters were estimated using the horizontal (parallel to the substratum) components of the gradients while the fluxes from the bulk liquid to the cell clusters and from the voids to the base film were calculated from the vertical (perpendicular to the substratum) components. The relative contribution of the diffusive oxygen fluxes across each of the three interfaces to the total flux was estimated by multiplying the flux by the corresponding interface area (from the observed structure). The area of each interface was based on a model with cylindrical cell clusters 170 μm high and diameters of 300 μm covering 50% of the substratum. Hence, over 1 m^2 of substratum there is a 0.5 m^2 void–base film interface (vertical flux), 0.5 m^2 bulk–cell cluster interface (vertical flux), and 1.13 m^2 void–cell cluster interface (horizontal flux). When U_{avg} was > 0.02 m/s the contribution of the voids to the

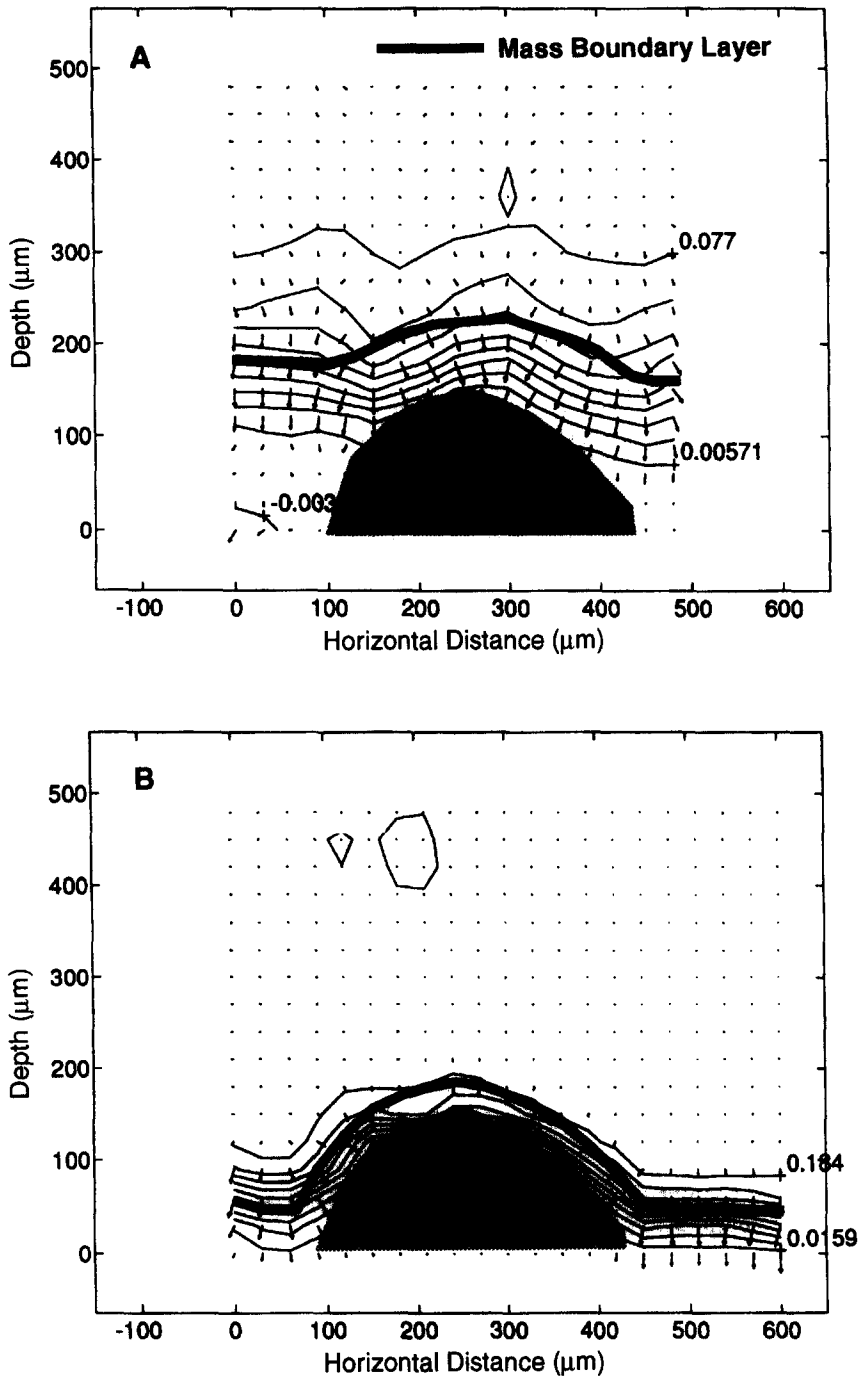

Fig. 3. Oxygen contour plots, measured at U_{avg} of 0.0078 m/s (A), and 0.115 m/s (B). The cell clusters and base film are shown in shading. The thin lines represent the oxygen contours, drawn at equal intervals of oxygen concentration. The numbers in the figure and on the right margin indicate local oxygen concentrations (mol/m^3). The thick solid line indicates the upper limit of the mass transfer boundary layer. The arrows show the direction of the largest oxygen gradients.

total mass transport was less than 50%, but when U_{avg} was increased to 0.04 m/s the oxygen transport from the voids to the cell clusters slightly exceeded the vertical fluxes, the total flux being about 6 mol/m^{2}s. At U_{avg} of 0.115 m/s transport from the voids to the cell clusters reached 60% of the total oxygen flux (about 17 mol/m^{2}s), thus the presence of voids increased the oxygen flux by a factor of about 2.5.

The presence of voids in biofilms has been associated with increased fluxes of substrates and products between the biofilm and the bulk liquid (Characklis *et al.*, 1990b; Eighmy *et al.*, 1983; Korber

et al., 1994; Kuhl and Jorgensen, 1992; Lawrence *et al.*, 1991). However, some of these studies were performed with very thin biofilms (3–40 μm) under very low flow velocities (0.0005 m/s, Re < 1) or the channels in the biofilm were as narrow as 1 μm. Our results indicate that under such conditions voids would not enhance mass transfer. Enhanced mass transport only occurs if the mass transfer boundary layer closely follows the irregular biofilm surface. The voids, then, facilitate convective mass transport which becomes increasingly significant at higher flow velocities.

CONCLUSIONS

(1) The mass transfer boundary layer is parallel to the substratum at low flow velocities, regardless of biofilm heterogeneity, but at higher flow velocities it closely follows the irregular biofilm surface. Hence, the effects of biofilm heterogeneity on mass transport are strongly dependant on the average flow velocity.

(2) Voids in biofilms can enhance the rates of substrate and product exchange with the bulk liquid by facilitating convection when the flow velocity is such that the mass transfer boundary layer closely follows the irregular biofilm surface. As the flow velocity increases past this critical point mass transport through the voids becomes increasingly significant.

(3) At low flow velocities heterogenous biofilms may be modeled as planar structures, with respect to mass transport, but at higher velocities more complex three-dimensional models may be more appropriate.

Acknowledgements—The research was supported by the cooperative agreement EEC-8907039 between the National Science Foundation and Montana State University. We thank Dr Philip Stewart for his valuable ideas, Brian Goldstein for data processing, and Peg Dirckx for editorial assistance.

REFERENCES

Bryers J. D. (1987) Processes governing the formation and persistence of biofilms. *Biotechnol. Prog.* **3,** 57–68.

Caldwell D. E., Korber D. R. and Lawrence J. R. (1992) Imaging of bacterial cells by fluorescence exclusion using scanning confocal laser microscopy. *J. Microb. Meth.* **15,** 249–261.

Characklis W. G. (1973) Attached microbial growth. II frictional resistance due to microbial slimes. *Water Res.* **7,** 1249–1258.

Characklis W. G., Turakhia M. H. and Zelver N. (1990a) Transport and interfacial transfer phenomena. In *Biofilms* (Edited by Characklis W. G. and Marshall K. C.), pp. 316–340. Wiley and sons, New York.

Characklis W. G., McFeters G. A. and Marshall K. C. (1990b) Physiological ecology in biofilm systems. In *Biofilms* (Edited by Characklis W. G. and Marshall K. C.), pp. 341–393. Wiley and sons, New York.

De Beer D., Stoodley P., Roe F. and Lewandowski Z. (1994a) Effects of biofilm structures on oxygen distribution and mass transport. *Biotechnol. Bioeng.* **43,** 1131–1138.

De Beer D., Stoodley P. and Lewandowski Z. (1994b) Liquid flow in heterogeneous biofilms. *Biotechnol. Bioeng.* **44,** 636–641.

Diks R. M. M. and Ottengraf S. P. P. (1991a) Verification studies of a simplified model for the removal of dichloromethane from waste gases using a biological trickling filter, Part I. *Bioproc. Eng.* **6,** 93–99.

Diks R. M. M. and Ottengraf S. P. P. (1991b) Verification studies of a simplified model for the removal of dichloromethane from waste gases using a biological trickling filter, Part II. *Bioproc. Eng.* **63,** 131–140.

Eighmy T. T., Maratea D. and Bishop P. L. (1983) Electron microscope examination of wastewater biofilm formation and structural components. *Appl. Environ. Microbiol.* **45**(6), 1921–1931.

Jorgensen B. B. and Des Marais D. J. (1990) The diffusive boundary layer of sediments: Oxygen microgradients over a microbial mat. *Limnol. Oceanogr.* **35**(6), 1343–1355.

Kashe V. and Kuhlman G. (1980) Direct measurement of the thickness of the unstirred diffusion layer outside immobilized biocatalysts. *Enzyme Microb. Technol.* **2,** 309–312.

Korber D. R., James G. A. and Costerton J. W. (1994) Evaluation of fleroxacin activity against established *Pseudomonas fluorescens* biofilms. *Appl. Environ. Microbiol.* **60**(5), 1663–1669.

Kuhl M. and Jorgensen B. B. (1992) Microsensor measurements of sulfate reduction and sulfide oxidation in compact microbial communities of aerobic biofilms. *Appl. Environ. Microbiol.* **58**(4), 1164–1174.

Lawrence J. R., Korber D. R., Hoyle B. D., Costerton J. W. and Caldwell D. E. (1991) Optical sectioning of microbial biofilms. *J. Bacteriol.* **173,** 6558–6567.

Lewandowski Z., Walser G. and Characklis W. G. (1991) Reaction kinetics in biofilms. *Biotechnol. Bioeng.* **38,** 877–882.

Massol-Deya A. A., Whallon J., Hickey R. F. and Tiedje J. M. (1995) Channel structures in aerobic biofilms of fixed-film reactors treating contaminated groundwater. *Appl. Environ. Microbiol.* **61**(2), 769–777.

Rittman B. E. and Manem J. A. (1992) Steady state, multispecies biofilm model. *Biotechnol. Bioeng.* **38,** 914–922.

Siegrist H. and Gujer W. (1985) Mass transfer mechanisms in a heterotrophic biofilm. *Water Res.* **19(11),** 1369–1378.

Skowland C. T. and Kirmse D. W. (1989) Simplified model for packed-bed biofilm reactors. *Biotechnol. Bioeng.* **33**(2), 164–172.

Stoodley P., De Beer D. and Lewandowski Z. (1994) Liquid flow in biofilm systems. *Appl. Environ. Microbiol.* **60**(8), 2711–2716.